

## Retraction

# Retracted: A Hemodynamic-Based Evaluation of Applying Different Types of Coronary Artery Bypass Grafts to Coronary Artery Aneurysms

### Complexity

Received 3 October 2023; Accepted 3 October 2023; Published 4 October 2023

Copyright © 2023 Complexity. This is an open access article distributed under the Creative Commons Attribution License, which permits unrestricted use, distribution, and reproduction in any medium, provided the original work is properly cited.

This article has been retracted by Hindawi following an investigation undertaken by the publisher [1]. This investigation has uncovered evidence of one or more of the following indicators of systematic manipulation of the publication process:

- (1) Discrepancies in scope
- (2) Discrepancies in the description of the research reported
- (3) Discrepancies between the availability of data and the research described
- (4) Inappropriate citations
- (5) Incoherent, meaningless and/or irrelevant content included in the article
- (6) Peer-review manipulation

The presence of these indicators undermines our confidence in the integrity of the article's content and we cannot, therefore, vouch for its reliability. Please note that this notice is intended solely to alert readers that the content of this article is unreliable. We have not investigated whether authors were aware of or involved in the systematic manipulation of the publication process.

Wiley and Hindawi regrets that the usual quality checks did not identify these issues before publication and have since put additional measures in place to safeguard research integrity.

We wish to credit our own Research Integrity and Research Publishing teams and anonymous and named external researchers and research integrity experts for contributing to this investigation.

The corresponding author, as the representative of all authors, has been given the opportunity to register their agreement or disagreement to this retraction. We have kept a record of any response received.

### References

- [1] H. Wang, H. Anzai, Y. Liu, A. Qiao, J. Xie, and M. Ohta, "A Hemodynamic-Based Evaluation of Applying Different Types of Coronary Artery Bypass Grafts to Coronary Artery Aneurysms," *Complexity*, vol. 2020, Article ID 9359340, 10 pages, 2020.

## Research Article

# A Hemodynamic-Based Evaluation of Applying Different Types of Coronary Artery Bypass Grafts to Coronary Artery Aneurysms

Haoran Wang,<sup>1,2</sup> Hitomi Anzai,<sup>1</sup> Youjun Liu,<sup>3</sup> Aike Qiao ,<sup>3</sup> Jinsheng Xie,<sup>4</sup> and Makoto Ohta <sup>1,2,5</sup>

<sup>1</sup>Institute of Fluid Science, Tohoku University, 2-1-1 Katahira, Aoba-ku, Sendai, Miyagi 980-8577, Japan

<sup>2</sup>Graduate School of Biomedical Engineering, Tohoku University, 6-6 Aramaki-aza-aoba, Aoba-ku, Sendai, Miyagi 980-8579, Japan

<sup>3</sup>College of Life Science and Bioengineering, Beijing University of Technology, No. 100, Pingleyuan, Chaoyang District, Beijing 100022, China

<sup>4</sup>Department of Cardiac Surgery, Beijing Anzhen Hospital, Capital Medical University, Beijing Institute of Heart Lung and Blood Vessel Diseases, Beijing 100029, China

<sup>5</sup>ELyTMaX UMI 3757, CNRS-Université de Lyon, Tohoku University, Sendai, Miyagi 980-8579, Japan

Correspondence should be addressed to Makoto Ohta; ohta@biofluid.ifs.tohoku.ac.jp

Received 28 March 2020; Revised 6 May 2020; Accepted 11 May 2020; Published 10 June 2020

Guest Editor: Zhihan Lv

Copyright © 2020 Haoran Wang et al. This is an open access article distributed under the Creative Commons Attribution License, which permits unrestricted use, distribution, and reproduction in any medium, provided the original work is properly cited.

Coronary artery bypass grafts (CABGs), including saphenous vein grafts (SVGs) or left internal mammary artery (LIMA) grafts, are recently applied to treat coronary artery aneurysm (CAA). Surgical outcomes are considered to be related to surgical strategies (types of the bypass graft and whether CAA ligated or not) and the size of the CAA (usually characterized by diameter). However, the understanding of the relationship between the surgical outcomes and the abovementioned factors is limited. Previous studies related to CABG treatments have shown hemodynamic studies could help evaluate surgical outcomes through graft mass flow rate, wall shear stress (WSS), and oscillatory shear index (OSI). It is believed that the hemodynamic study of applying CABGs to CAA, which is not studied yet, could help us understand the different CABG surgeries. The aim of the study was to evaluate the hemodynamic differences among different surgical methods. To do this, eight three-dimensional models were constructed, representing application of SVGs and LIMA grafts to CAAs (whether ligated or not) with diameters two, three, and five times the normal diameter, to perform computational fluid dynamics (CFD) simulation. The lumped-parameter model (LPM) was coupled to the boundary of the 3D models which increase the complexity of the simulation, but it can ensure the stability of the simulation boundary conditions. The results show that SVG (no matter whether ligated or not) hemodynamic characteristics are positive, with an average high graft mass flow rate of 70 ml/min, an average WSS of 0.479 Pa, and a low OSI of 0.001. LIMA with CAA ligation has the same characteristics with higher WSS (average 1.701 Pa). The hemodynamic characteristics of LIMA without CAA ligation are negative, including high reverse mass flow rate and high OSI (0.367). The results indicate that the surgical outcomes of LIMA with CAA ligation are likely to be the best among these models. The surgical outcomes of LIMA without CAA ligation seem to be undesirable due to the high reverse mass flow and high OSI. The CAA diameter may not have a significant effect on surgical outcomes.

## 1. Introduction

Coronary artery aneurysms (CAAs) are cardiovascular disease, which is defined as dilatation of the coronary artery exceeding more than 50% of the reference vessel diameter, and the incidence rate is approximately 0.3–5.3% [1, 2]. It

was learned that up to one-third of CAAs are associated with obstructive coronary artery disease and have been associated with myocardial infarction, arrhythmias, or sudden cardiac death [3]. Recently, coronary artery bypass graft (CABG) surgery is usually selected to treat myocardial ischemia and complications caused by CAAs [4–6]. However, because of

the rarity of CAA and the variety of surgeries, our understanding of applying CABGs to CAA is limited, most of which comes from case reports [7–11]. With the increase in patients and more and more applications of surgery, it is necessary to conduct a research on applying CABGs to CAA to help us understand the surgery.

There are usually two different surgical options and an important parameter to be considered when implementing CABG applying to CAA. The different surgical options include the types of CABGs and whether the CAA is ligated or not. Saphenous vein grafts (SVG) and left internal mammary artery (LIMA) grafts, harvested from the patients' own body, are the main choice for the bypass graft of CABG surgery [12]. SVG and LIMA have their own advantages and disadvantages, and there is no uniform standard. However, the SVG is the most widely used. Compared with LIMA, the SVG has the advantage of ease of use, sufficient length, and accessibility. Especially, for patients with a diffusely atherosclerotic ascending aorta, SVG composite Y-grafts may be necessary, particularly when there is some contraindication to the use of arterial grafts and severe (>70%) stenosis [13–15]. The CAA ligated or nonligated can cause different degrees of damage to blood vessels. Ligation is to cut off the original coronary arteries, which will cause huge structural damage to the cardiovascular system. Without ligation, it will only cause anastomotic damage and no other structural damage. The important parameter to be considered is the size of the CAA, which is usually characterized by diameter. Changes in the size of the CAA diameter could affect the complications, which means the surgical strategy may be affected.

To the best of our knowledge, because of scarcity of CAA and complexity of factors affecting the surgical outcomes of surgery, there are no research studies conducted on applying CABGs to CAA to investigate the differences in surgical outcomes caused by different types of bypass grafts, CAA ligated or not. The effect of CAA diameter on different surgical methods is also unknown. The study of hemodynamics provides an effective method for us to solve the abovementioned problems. Previous studies have pointed out that hemodynamic study of applying CABGs to treat other diseases such as coronary stenosis by using computational fluid dynamics (CFD), which has attracted wide attention in recent years and has many applications in the vascular field [16–18], has made progress. Also, those research studies confirm that surgical outcomes correlate with some important hemodynamic characteristics including mass flow rate, wall shear stress (WSS), and oscillatory shear index (OSI) [19–24]. Therefore, it is reasonable to believe that hemodynamic study of applying CABGs to CAA can be used to evaluate the surgical outcomes.

The aim of this study was to evaluate the hemodynamic differences between two different surgical methods (types of CABGs, whether CAA ligated or not) and the effect of CAA diameter on the hemodynamics of different surgical methods through the CFD method. It could allow us to evaluate different surgical procedures of CAA and make preliminary predictions and deduction for different surgical plans based on these hemodynamic characteristics from a

hemodynamic perspective. This research may be the first hemodynamic study that evaluates the hemodynamic characteristics of different types of bypass grafts on CAA of different diameters and makes a rank of treatment procedure based on the hemodynamic characteristics. This study may provide information to clinicians for better predicting of surgery and making more reliable treatment decisions.

## 2. Materials and Methods

**2.1. Model Development.** A patient-specific 3D geometric anatomical model was reconstructed based on medical images that were obtained by computed tomography angiography (CTA, Siemens). The CTA images of the patient, whose information was anonymized in this research, were provided by Anzhen Hospital with  $512 \times 512$  pixels of each image, 450 slice images, and 1 mm gap between adjacent slice. This study has been approved by the Medical Ethics Committee of Beijing Anzhen Hospital and Tohoku University. The construction processing of the 3D model was done by using Mimics (Materialise NV, BE) through both manual and threshold segmentation. Three different diameters of CAA, including the diameters of two, three, and five times compared with the adjacent coronary artery, were applied to the left anterior descending artery by using Geomagic Freeform (3D system, US) software. Virtual bypass surgery was implemented on these models including SVG and LIMA bypass grafts. Two more virtual bypass surgery models (SVG and LIMA) in which CAA was ligated were also established. Figure 1 shows the details of all different 3D models which were named model 1–8, respectively.

**2.2. Computational Model and Properties of Fluid.** The finite element analysis method will be adopted in which all models need to be preprocessed, including preprocessing of the inlets and outlets and the smooth processing of the area of interest. Preprocessing models need to be divided into meshes, which were hexahedral meshes that were controlled by means of size control with the software ANSYS Meshing (ANSYS, US), to generate the fluid computational models. The mesh of the area of interest is refined in order to get more accurate results in these areas. The mesh independency was analyzed to guarantee the reliability of the simulation results, which needed the number of elements and nodes to be large enough [25]. Table 1 shows the results of the mesh independency test. The differences in WSS between the chosen mesh were less than 0.5%. The calculation result can be considered stable. Table 2 shows the details of the number of elements and nodes of all 8 models in this paper. Blood flow simulations were performed with the ANSYS-CFX (ANSYS, US) Navier–Stokes solver. In the simulation, we assumed that the wall was rigid and stationary. This study assumed that blood was an incompressible Newtonian fluid with a viscosity of  $0.0035 \text{ Pa}\cdot\text{s}$  and a density of  $1050 \text{ kg/m}^3$ . Simulations were run for 3 cardiac cycles. We selected  $0.0025 \text{ s}$  time step to satisfy the calculation of stability conditions. The maximum convergence RMS residual of simulation was set to 0.0001.

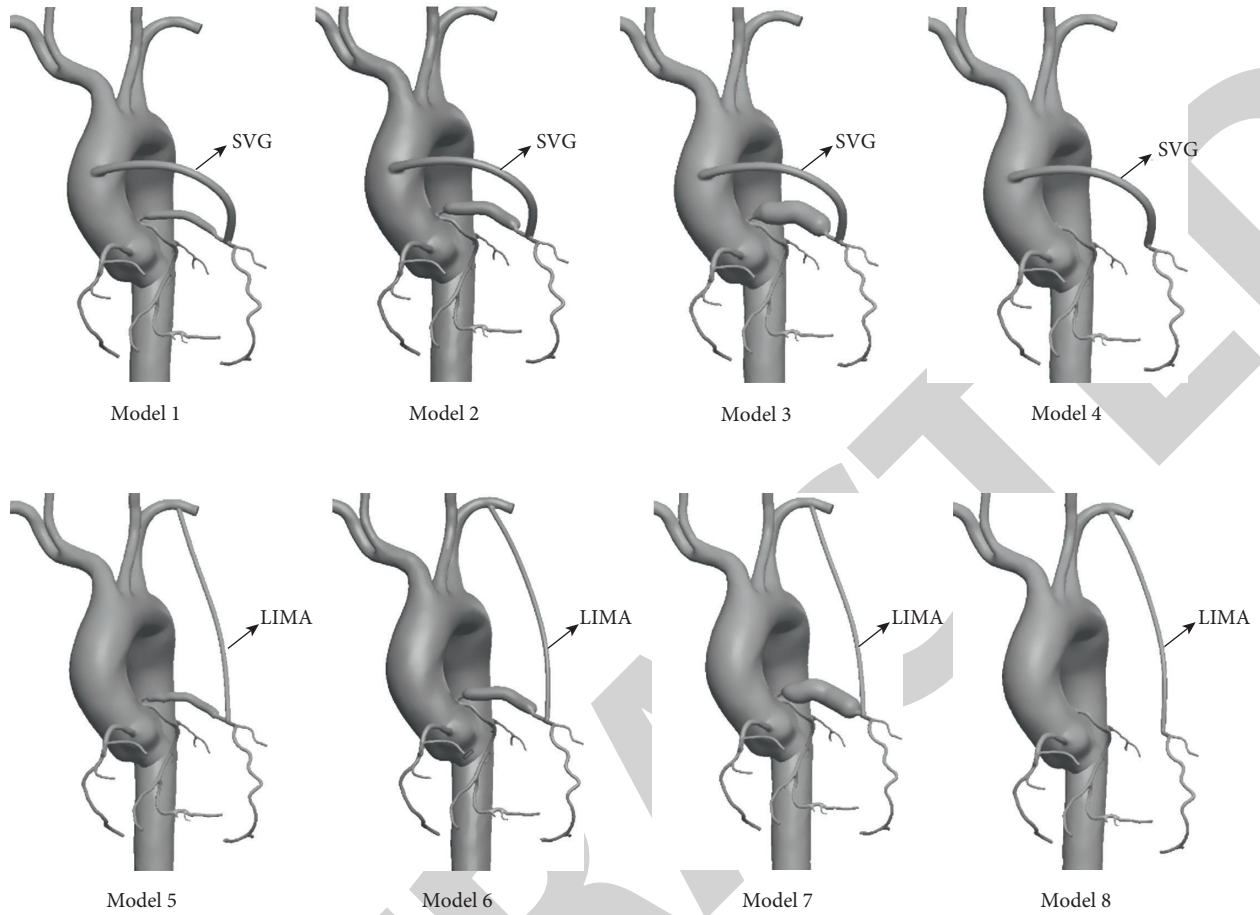


FIGURE 1: All eight 3D CABG surgery models which describe the location and the size of the CAA and the way of how to perform the bypass surgery. Models 1–4: bypass graft is SVG and the diameter of CAA is 2x, 3x, 5x, and 0 (CAA ligated), separately. Models 5–8: bypass graft is LIMA and the diameter of CAA is 2x, 3x, 5x, and 0 (CAA ligated), separately.

TABLE 1: The results of the mesh independency test on WSS and pressure.

| Number of meshes | Percent change of the parameter values | SVG            |                  | LIMA           |                 |
|------------------|--|----------------|------------------|----------------|-----------------|
|                  |  | WSS (Pa)       | Pressure (mmHg)  | WSS (Pa)       | Pressure (Pa)   |
| 200,000          |  | 0.626          | 77.912           | 0.639          | 79.038          |
| 400,000          | $\epsilon$                             | 0.599<br>4.30% | 86.293<br>10.70% | 0.623<br>2.50% | 86.395<br>9.30% |
| 600,000          | $\epsilon$                             | 0.621<br>3.60% | 82.629<br>4.20%  | 0.62<br>0.50%  | 82.547<br>4.50% |
| 800,000          | $\epsilon$                             | 0.61<br>1.80%  | 84.324<br>2.00%  | 0.608<br>1.90% | 84.672<br>2.60% |
| 1,000,000        | $\epsilon$                             | 0.607<br>0.50% | 84.197<br>0.20%  | 0.609<br>0.16% | 84.925<br>0.30% |

$\epsilon$  is the percentage change of the parameter value (WSS and pressure) due to the increase in the number of meshes.

**2.3. Boundary Conditions: Lumped-Parameter Model Boundary Conditions.** Boundary conditions of computational simulation play an important role that can affect the accuracy of the results and determine whether the calculation is successful. The ideal situation is to obtain the real human beings' physiological parameters as the boundary conditions of the simulation calculation. However, obtaining coronary artery physiological parameters is not easy due

to its small size, numerous branches, and distribution on the heart's surface. Therefore, in order to obtain life-like boundary conditions, we selected the lumped-parameter model (LPM), which is a circuit model that can simulate the blood flow and pressure through current and voltage, to provide boundary conditions for the CFD simulation [25–27]. One reason for choosing LPM is its simplicity. Complex coronary branches can be simulated by simple

TABLE 2: The values of nodes and elements of all models.

|          | Model 1   | Model 2   | Model 3   | Model 4   | Model 5   | Model 6   | Model 7   | Model 8   |
|----------|-----------|-----------|-----------|-----------|-----------|-----------|-----------|-----------|
| Nodes    | 1,007,389 | 1,016,509 | 1,145,628 | 1,003,758 | 1,004,659 | 1,018,965 | 1,159,365 | 1,007,932 |
| Elements | 1,238,694 | 1,335,889 | 1,369,378 | 1,218,463 | 1,239,574 | 1,339,365 | 1,359,436 | 1,228,346 |

circuit modules while retaining the characteristics of coronary blood supply. On the other hand, less demand for computing resources, which means better adaptability and lower consumption, is meaningful.

LPM consists of three modules, which are arterial module, coronary module, and heart module. The arterial module consists of many branches which base a three-element model (Windkessel RCR model) [28] structure that consists of two resistors and one capacitor. The coronary module consists of the arterial module and coronary microcirculation module. The main feature of coronary microcirculation is the resistance to drastic changes caused by the contraction of the heart. The myocardial compliance ( $C_{i-micro}$ ) and microcirculation resistance ( $R_{v-micro}$ ) were used to simulate this feature, where the cathode of the capacitor is loaded with intramyocardial pressure to simulate the pressure generated by the contraction of the heart during the systolic phase. In the LPM heart model, all the simulation equations of the left ventricle is based on the previous research [25] including  $C(t)$ ,  $E(t)$ ,  $E_{max}$ ,  $E_{min}$ ,  $E_n(t_n)$ , and  $t_n$ , and we determined the specific value of each component including resistors and capacitors, which are adjusted to match the patient's blood pressure.

Based on the abovementioned 0D model and 3D models, the multiscale 0D/3D coupling model used in this research was constructed. Figure 2 shows coupling interface details of the 0D/3D coupling model. All 3D models were coupled with the same 0D model whose parameter values adopt the values of the normalized coronary model, which is confirmed by observing that the geometric structure of the distal coronary artery was not changed. Models sharing the same LPM can also exclude other factors to ensure that the change of the values of hemodynamic parameters is only related to the geometric structure.

**2.4. Hemodynamic Parameters.** Hemodynamics can reveal the characteristics of the blood flow. We will focus on several key hemodynamic parameters including mass flow rate, WSS, and OSI. The WSS represents the force per unit area of fluid applied along the wall surface in the direction of the local tangent plane [29]. Formula (1) is as follows:

$$WSS = \tau_w = \mu \left( \frac{\partial u}{\partial y} \right)_{y=0}, \quad (1)$$

where  $\mu$  is the dynamic viscosity,  $u$  is the velocity parallel to the wall, and  $y$  is the distance to the wall. OSI quantifies WSS direction changes. OSI is calculated using the following formula:

$$OSI = \frac{1}{2} \left( 1 - \frac{\left| \int_0^T \vec{\tau}_w dt \right|}{\int_0^T |\vec{\tau}_w| dt} \right). \quad (2)$$

### 3. Results

In this finite element simulation, we evaluated some key hemodynamic parameters which could help evaluate surgery, including mass flow rate, WSS, and OSI on the bypass graft.

**3.1. Mass Flow and Pressure Drop.** The values of mass flow through the bypass grafts and the pressure difference between the upstream and downstream of the bypass grafts over a cardiac cycle are shown in Figure 3. The results show that the mass flow rate of the SVG (no matter) is much higher than that of LIMA, in which the peak value is up to 120 ml/min and the mean value is 50 ml/min, except the LIMA model with ligation of CAA. The mass flow rate of the LIMA in model 8 with ligation of CAA is almost the same as that of the SVGs. The mean mass flow rate of the LIMA in models 5–7 without ligation of CAA is almost 0. The reverse flow which means the blood flows from the bottom to the top of the LIMA can be found in these models without ligation of CAA during the systolic phase of the heart. The negative pressure difference is found in the LIMA models without CAA ligation (models 5–7), while the pressure difference of other models is always positive. Pressure difference is the main driving force of liquid in fluid simulation, which may indicate the main cause of the reverse flow.

**3.2. Wall Shear Stress.** WSS is a force applied to a tangent plane which indicates the per unit area force exerted by the fluid [30]. The values of WSS on SVGs and LIMAs of all models over a cycle and WSS distribution on the SVGs and LIMAs of all models (peak point) are shown in Figures 4 and 5. The mean area WSS on the bypass grafts of models 1–8 over a cycle is 0.477, 0.483, 0.516, 0.443, 0.851, 0.877, 0.896, and 1.701 Pa, respectively. Under the same conditions, WSS on the LIMA is higher than that of the SVG. WSS on the LIMA with CAA ligation (model 8) is especially higher.

**3.3. Oscillatory Shear Index.** OSI is a parameter that can quantify the change in direction and magnitude of the WSS [31]. The distribution of OSI on all models is shown in Figure 6. The mean area values of OSI on SVGs and LIMAs of all models are 0.001, 0.001, 0.001, 0.001, 0.343, 0.281, 0.476, and 0.001, respectively. The values of OSI on SVGs (no matter whether CAA is ligated or not, models 1–4) and the values of OSI on LIMA with CAA ligation (model 8) are almost 0 which means the direction of blood flow has almost no change. In contrast, the values of OSI on LIMAs without CAA ligation (models 5–7) are decades of orders of magnitude higher than the same condition of SVGs (no matter whether CAA is ligated or not).

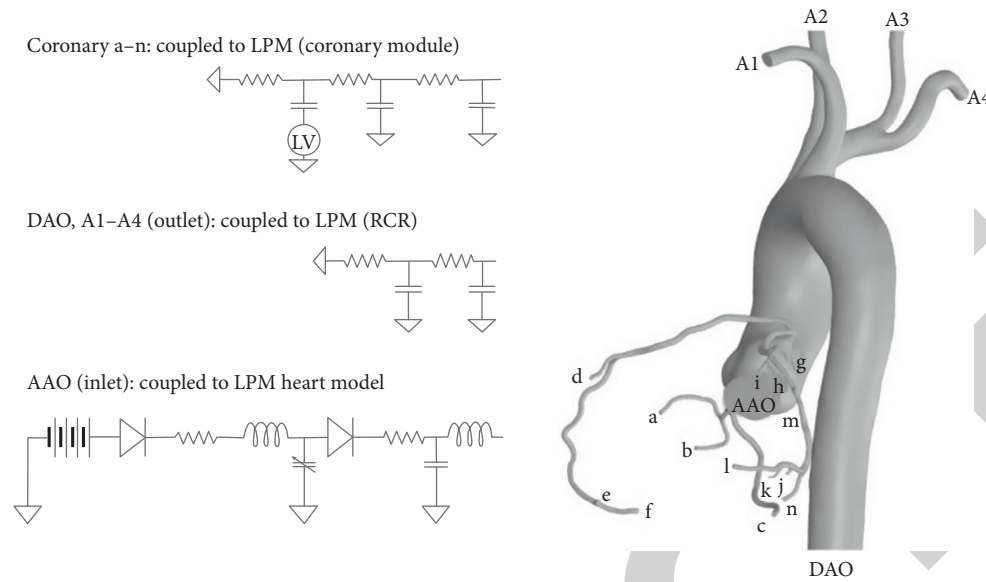


FIGURE 2: The construction of interfaces of the 0D/3D coupling model. In the coupled system, the coronary module of LPM is coupled with the coronary arteries of the 3D model, the LPM heart module is coupled with the aortic inlet of the 3D model, and the common artery LPM module (RCR) is coupled with other branch arteries of the 3D model.

#### 4. Discussion

CABG (including SVG and LIMA) surgical operation nowadays is generally selected to treat CAA. Moreover, whether CAA is ligated or not is another choice. Surgical outcomes differ depending on the types of bypass grafts and diameter of CAA (ligated or not). Hemodynamic characteristics (mass flow rate, WSS, and OSI) of different types of CABG surgeries (SVG and LIMA) applied to CAA (different diameters, ligated or not), which were related to surgical outcomes based on the previous studies, are obtained through the CFD method.

We found that the hemodynamics of CAA ligation models is better than those of models without CAA ligation. When CAA was not ligated, the SVG has better hemodynamic characteristics than LIMA. When the same type of bypass graft is used, the change of CAA diameter has basically no effect on the hemodynamic characteristics of the bypass graft.

We deduced that surgical outcomes of LIMA with CAA ligation may be the best and surgical outcomes of the SVG may be superior to LIMA without CAA ligation. Surgical methods, including the type of bypass graft and CAA ligated or not, may be the main factors affecting the outcomes of the operation, and CAA diameter could be a minor factor.

##### 4.1. Characteristics of Mass Flow Rate of Bypass Grafts.

Mass flow rate, which is one of the few parameters that can be measured directly during the procedure, is one of the key hemodynamic parameters for clinical surgery. Most of the time, this indicator is the most direct indicator for judging the success of surgery [19, 32]. There are no significant differences in the mass flow rate of SVG between different diameters of CAA. The mass flow curves of SVG with and

without CAA ligation are similar in which the minimum and maximum values are 50 ml/min and 120 ml/min. The mass flow curves of LIMA models 5–7, without CAA ligation, are similar in which the minimum and maximum values are  $-50$  ml/min and 60 ml/min. There is significant reverse flow during the systolic phase. Studies have shown that reverse flow is harmful to bypass grafts and is associated with the string phenomenon which indicates the failure of the bypass grafts [19, 20]. A reverse flow value of  $\geq 3.0\%$  can be considered as a cutoff value that predicts early graft failure [20]. The reverse flow value of 43.5% without CAA ligation is much higher than 3.0% in this research. Therefore, early graft failure may happen in LIMA without CAA ligation. However, by comparison, mass flow rate of LIMA with CAA ligation is much higher than that of LIMA without CAA ligation, in which the minimum and maximum values are 30 ml/min and 100 ml/min and no reverse flow exists. Mass flow rates of SVGs with and without CAA ligation and LIMA with CAA ligation are usually the expected results which are with higher mass flow and no reverse flow.

The inlet locations and the diameters of the grafts are the major geometrical differences between SVG and LIMA grafts in this research. On the one hand, the inlet of an SVG is closer to the aortic root than that of an LIMA graft. Therefore, the pressure delay of SVGs is less than that of LIMAs. On the other hand, the location close to the aortic root ensures that the pressure upstream of the bypass graft is close to the aortic pressure which can keep the pressure difference between the upstream and downstream of the bypass graft positive. The inlet of the LIMA is far from the root of the aorta which caused a negative pressure difference across the LIMA. The pressure difference has been shown in Figure 3 which can confirm our point of view. Except for LIMA without CAA ligation, the pressure difference of the bypass grafts in other models is always positive in the cardiac

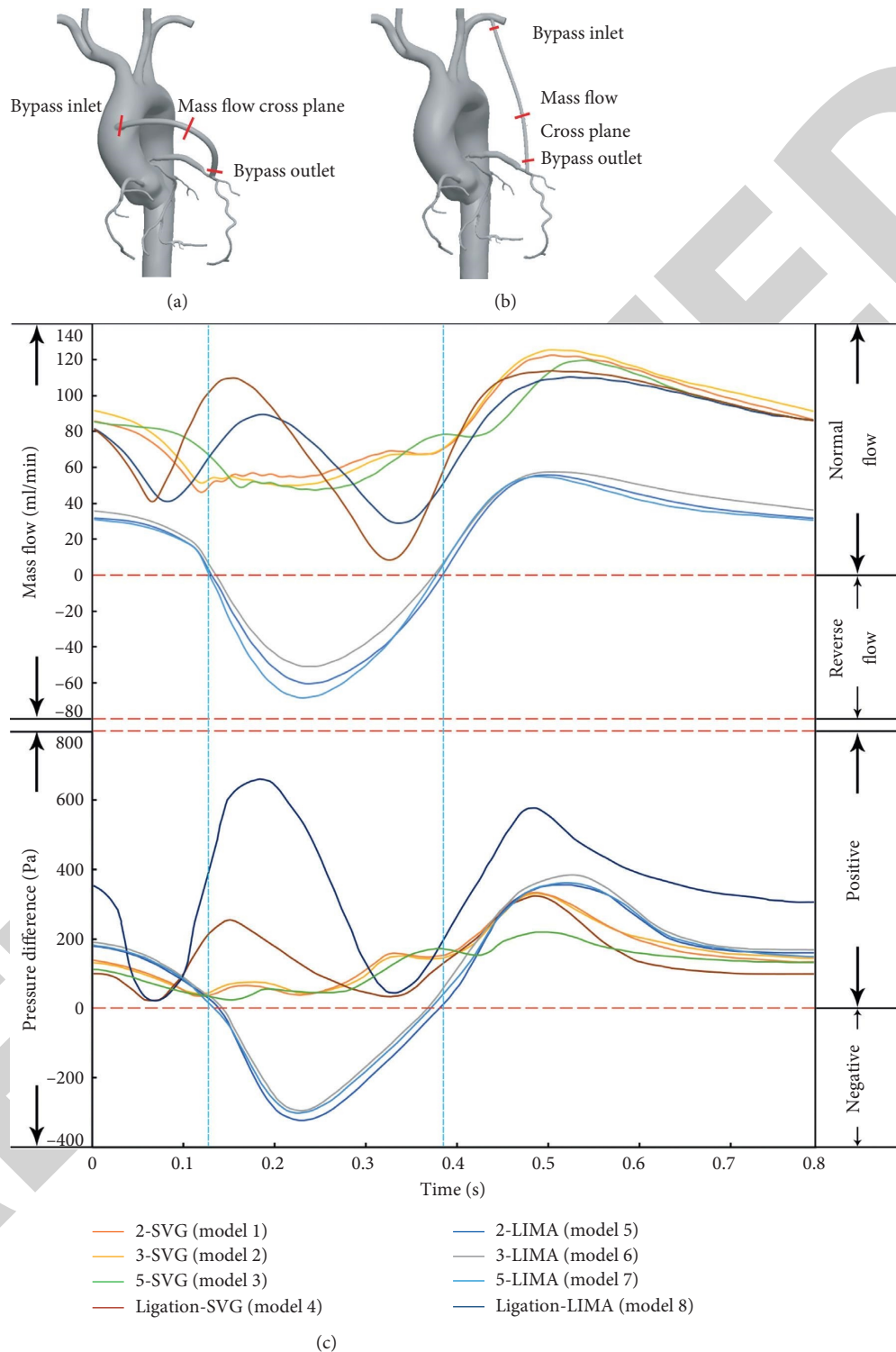


FIGURE 3: The mass flow rate depending on times of the bypass grafts through the cross plane and the pressure difference between the bypass inlet and the bypass outlet. (a) Representation of the SVG virtual surgery model and three locations on the SVG. (b) Representation of the LIMA virtual surgery model and three locations on the LIMA. (c) The mass flow rate through the cross plane of the bypass grafts in all models, as shown in (a) and (b), and the pressure difference between the bypass inlet and bypass outlet in all models, as shown in (a) and (b).

cycle. In the models of LIMA without CAA ligation, the significant negative pressure difference was found which might be the major reason for the reverse flow during the

systole period in an LIMA graft. A larger diameter means less resistance. This may be the main reason why the mass flow of SVG is higher than that of LIMA with CAA ligation.

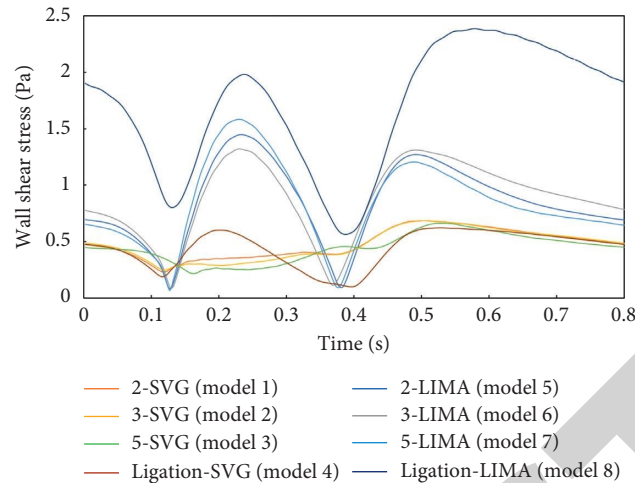


FIGURE 4: The WSS depending on times of the bypass grafts (SVG and LIMA) in a cardiac cycle.

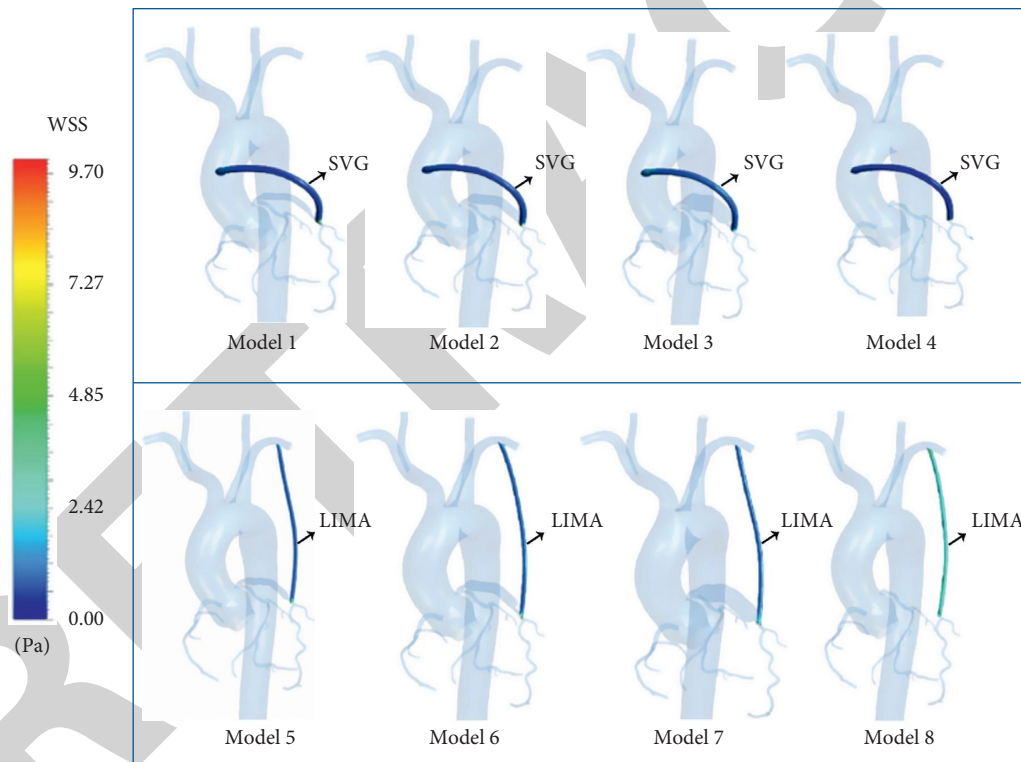


FIGURE 5: The WSS distribution on the bypass grafts (SVG and LIMA) at the peak point ( $t=0.24$  s) in a cardiac cycle.

**4.2. Characteristics of WSS of Bypass Grafts.** WSS is related to some important physiological processes of endothelial cells, such as the formation of important compounds [21, 22]. According to previous research including simulation and experimental research, WSS values have different effects on physiological processes of endothelial cells when they are in different ranges. According to the experimental reports, the results from experiments in parallel-plate flow chambers revealed that a low WSS value of 0.4 Pa induced extensive platelet aggregation [33]. This

abnormal behavior is considered to have the potential to cause vascular diseases. The simulation study also reached a similar conclusion, that is, when the WSS is less than 0.4 Pa, the blood vessels are prone to lesions [34, 35]. Simulation studies also found that the WSS interval which maintains normal physiological functions of blood vessels is generally considered to be 1–7 Pa. WSS values ranging from 0.4–1 Pa is usually considered a transition zone where the trend of blood vessel development cannot be easily predicted. Therefore, even if the WSS is greater than 0.4, we cannot

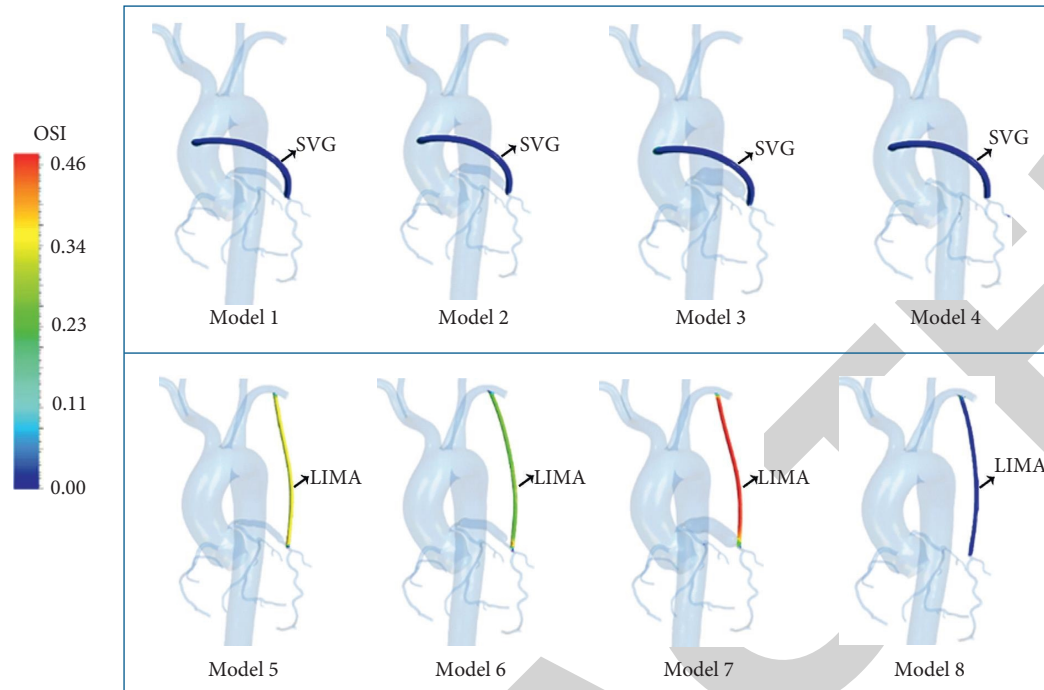


FIGURE 6: The OSI distribution on the bypass grafts (SVG and LIMA) in a cardiac cycle.

guarantee that the function of the blood vessels will not be affected at all. Our research results are as follows. WSS in SVGs (with and without CAA ligation, models 1–4) is similar, with an average value of 0.479 Pa. WSS in LIMAs (without CAA ligation, models 5–7) is similar, with an average value of 0.874 Pa. WSS in LIMA (with CAA ligation, model 8) is much higher, with a value of 1.701 Pa. In the simulation results, only the WSS value in LIMA with CAA ligation is in the range of 1–7 Pa and all others are in the range of 0.4–1 Pa. Therefore, LIMA with CAA ligation may be most in line with expectations. WSS values in other methods are not the best, but the results are still acceptable.

**4.3. Characteristics of OSI of Bypass Grafts.** OSI is used to reveal the degree of WSS vector direction change which can help us understand the oscillation information of blood flow [36]. Simulation studies have pointed out that low OSI may reduce the risk of graft failure [23, 24]. *In vitro* studies using bovine endothelial cells revealed that slowly oscillating (1 Hz) shear stress (equal to the upper limit of OSI of 0.5) induced the expression of monocyte chemoattractant protein-1 and increased binding of monocytes to the endothelium which indicate high OSI has the potential to increase the risk of vascular failures [37]. Smaller OSI means more stable blood flow and better guarantee of blood vessel stability. The simulation results of this study showed that OSI in all SVGs (with and without CAA ligation) is quite small and close to 0. OSI in LIMA (without CAA ligation, models 5–7) is quite high with an average value of 0.367. OSI in LIMA (with CAA ligation, model 8) is quite small which is close to 0. The results of different surgical methods are significantly different. OSI levels are two orders of magnitude lower in the

SVG with and without CAA ligation than LIMA without CAA ligation. LIMA with CAA ligation has similar condition as the SVG. Therefore, the simulation results of the SVG and LIMA with CAA ligation are in line with the target. LIMA without CAA ligation is at risk due to too high risk of failure.

**4.4. Summing-Up and Deduction.** As mentioned above, we extracted and analyzed three key hemodynamic parameters including mass flow rate, WSS, and OSI. The results show that high mass flow rate, relatively low WSS, and low OSI (almost 0) are the main features for the SVG with and without CAA ligation. Low mass flow rate, low WSS, and high OSI are the main features for the LIMA without CAA ligation. In contrast, high mass flow rate, high WSS, and low OSI (almost 0) are the main features for the LIMA with CAA ligation. The results show that changes in CAA diameter have no significant effect on hemodynamic features of the same category. According to previous research, achieving high mass flow, high WSS, and low OSI to reduce adverse hemodynamic factors is important, in order to reduce the risk of surgical failure and prolonging long-term effectiveness of the graft. Among the several surgical methods in this study, LIMA with CAA ligation has the optimal hemodynamic parameters compared with other models. SVG with and without CAA ligation have similar hemodynamic conditions which are all anticipated apart from the relatively low WSS. LIMA without CAA ligation has negative hemodynamic parameter results that are not expected. Based on our hemodynamic results, we deduced that surgical outcomes may have nothing to do with CAA diameter. LIMA with CAA ligation may have the best surgical

outcomes, and SVG (both with and without CAA ligation) surgical outcomes are better than that of LIMA without CAA ligation. LIMA without CAA ligation may not be desirable. When a coronary artery is ligated, it means that the blood supply to this branch is completely cut off. The blood supply at this time can only rely on the bypass grafts. Once the bypass grafts have problems, the blood vessels themselves cannot perform compensatory adjustments in time which originally can be performed without ligation. Therefore, even though CABGs with CAA ligation may have better surgical outcomes, we need to be very careful with this surgical approach due to other potential risks.

**4.5. Limitations of the Work.** An important limitation of this study is the number of patients. The model in this study was only based on one patient's data, so the results of the study may be special and accidental. The second limitation is the assumption of rigid arterial walls in the simulation, which does not account for the significant motion and curvature changes of the coronary arteries and bypass grafts during the cardiac cycle. In addition, rigid arterial walls mean that the effect of material deformation on blood flow is ignored. This problem can be solved by adopting a fluid-solid interaction (FSI) method in the future. An additional limitation is limited data on flow split percentages to the left and right coronary arteries and the relationship between the intramyocardial pressures to the left and right ventricular pressures, and these are possible minor sources of error during building the LPM.

## 5. Conclusion

In this paper, the hemodynamic differences between two different surgical methods (types of CABGs, whether CAA ligated or not) and the effect of CAA diameter on the hemodynamics of different surgical methods were compared by using CFD simulation. A hemodynamic-based evaluation of these procedures was performed. The results suggest that LIMA with CAA ligation has the best hemodynamic characteristics, including high mass flow rate, high WSS, and low OSI. Hemodynamic characteristics of the SVG (with and without CAA ligation) are better than those of the LIMAs without CAA ligation including high mass flow rate, WSS, and low OSI. Significant reverse flow that can increase the risk of graft failure was found in LIMAs without CAA ligation during systole. The change of CAA diameter has basically no effect on the hemodynamics of the same bypass graft. Based on the previous hemodynamic research, we deduced that the outcomes of ligation surgery may have more benefits than those of nonligation surgery. SVG may be a better choice than LIMA when CAA is not ligated. This preliminary result warrants extensive research involving a larger aneurysm database for further analysis.

## Data Availability

The data used to support the findings of this study are available from the corresponding author upon request.

## Conflicts of Interest

The authors declare no conflicts of interest.

## Acknowledgments

This research was supported by the National Natural Science Foundation of China (nos. 11832003 and 11772016), and JSPS KAKENHI (no. JP18K18355). This research was partially supported by the creation of a development platform for implantable/wearable medical devices by a novel physiological data integration system of the Program on Open Innovation Platform with Enterprises, Research Institute and Academia (OPERA) from the Japan Science and Technology Agency (JST).

## References

- [1] M. Syed and M. Lesch, "Coronary artery aneurysm: a review," *Progress in cardiovascular diseases*, vol. 40, no. 1, pp. 77–84, 1997.
- [2] S. Abou Sherif, O. Ozden Tok, Ö. Taşköylü, O. Goktekin, and I. D. Kiliç, "Coronary artery aneurysms: a review of the epidemiology, pathophysiology, diagnosis, and treatment," *Frontiers in Cardiovascular Medicine*, vol. 4, 2017.
- [3] C. Indolfi, F. Achille, G. Tagliamonte, C. Spaccarotella, A. Mongiardo, and A. Ferraro, "Polytetrafluoroethylene stent deployment for a left anterior descending coronary aneurysm complicated by late acute anterior myocardial infarction," *Circulation*, vol. 112, no. 5, pp. 70–71, 2005.
- [4] K. G. Friedman, K. Gauvreau, A. Hamaoka-Okamoto et al., "Coronary artery aneurysms in kawasaki disease: risk factors for progressive disease and adverse cardiac events in the US population," *Journal of the American Heart Association*, vol. 5, no. 9, 2016.
- [5] S. K. Singh, T. Goyal, R. Sethi et al., "Surgical treatment for coronary artery aneurysm: a single-centre experience," *Interactive Cardiovascular and Thoracic Surgery*, vol. 17, no. 4, pp. 632–636, 2013.
- [6] E. Beckmann, S. Rustum, S. Marquardt et al., "Surgical treatment of coronary artery aneurysms," *Journal of Cardiac Surgery*, vol. 32, no. 11, pp. 674–679, 2017.
- [7] J. E. Markis, C. D. Joffe, P. F. Cohn, D. J. Feen, M. V. Herman, and R. Gorlin, "Clinical significance of coronary arterial ectasia," *The American Journal of Cardiology*, vol. 37, no. 2, pp. 217–222, 1976.
- [8] J. Hillebrand, A. Rukosujew, S. Martens, and D. Boese, "Redo operation of recurrent giant coronary artery aneurysm: optimizing surgical strategy," *The Thoracic and Cardiovascular Surgeon Reports*, vol. 5, no. 1, pp. 57–59, 2016.
- [9] A. Dolapoglu and D. A. Ott, "Giant right coronary artery aneurysm associated with a fistula draining into the superior vena cava," *Texas Heart Institute Journal*, vol. 43, no. 4, pp. 360–362, 2016.
- [10] A. Naraen, P. Reddy, C. Notarstefano, and M. Kudavali, "Giant coronary artery aneurysm in a middle-aged woman," *The Annals of Thoracic Surgery*, vol. 103, pp. 313–315, 2017.
- [11] S. Komoda, T. Komoda, E. Ivanitskaia-Kuehn, S. Dreyse, M. Pasic, and R. Hetzer, "Giant aneurysm of the right coronary artery and fistula to the coronary sinus," *General Thoracic and Cardiovascular Surgery*, vol. 58, no. 2, pp. 78–81, 2010.

- [12] M. Gaudino, D. Taggart, H. Suma, J. D. Puskas, F. Crea, and M. Massetti, "The choice of conduits in coronary artery bypass surgery," *Journal of the American College of Cardiology*, vol. 66, no. 15, pp. 1729–1737, 2015.
- [13] J.-H. Wi, H.-C. Joo, Y.-N. Youn, S.-W. Song, T. H. Kim, and K.-J. Yoo, "Comparison of radial artery and saphenous vein composite  $\gamma$  grafts during off-pump coronary artery bypass," *The Korean Journal of Thoracic and Cardiovascular Surgery*, vol. 46, no. 4, pp. 265–273, 2013.
- [14] H. A. Al-Sabti, A. Al Kindi, K. Al-Rasadi, Y. Banerjee, K. Al-Hashmi, and A. Al-Hinai, "Saphenous vein graft vs. radial artery graft searching for the best second coronary artery bypass graft," *Journal of the Saudi Heart Association*, vol. 25, no. 4, pp. 247–254, 2013.
- [15] N. G. Baikoussis, N. A. Papakonstantinou, and E. Apostolakis, "Radial artery as graft for coronary artery bypass surgery: advantages and disadvantages for its usage focused on structural and biological characteristics," *Journal of Cardiology*, vol. 63, no. 5, pp. 321–328, 2014.
- [16] H. Anzai, T. Watanabe, X. Han et al., "Endothelial cell distributions and migration under conditions of flow shear stress around a stent wire," *Technology and Healthcare*, 2019, in Press.
- [17] H. Anzai, B. Chopard, and M. Ohta, "Combinational optimization of strut placement for intracranial stent using a realistic aneurysm," *Journal of Flow Control, Measurement & Visualization*, vol. 2, no. 2, pp. 67–77, 2014.
- [18] M. Zhang, Y. Li, X. Zhao et al., "Haemodynamic effects of stent diameter and compaction ratio on flow-diversion treatment of intracranial aneurysms: a numerical study of a successful and an unsuccessful case," *Journal of Biomechanics*, vol. 58, pp. 179–186, 2017.
- [19] D. K. H. Leong, V. Ashok, A. Nishkantha, Y. H. Shan, and E. K. W. Sim, "Transit-time flow measurement is essential in coronary artery bypass grafting," *The Annals of Thoracic Surgery*, vol. 79, no. 3, pp. 854–857, 2005.
- [20] K. Honda, Y. Okamura, Y. Nishimura et al., "Graft flow assessment using a transit time flow meter in fractional flow reserve-guided coronary artery bypass surgery," *The Journal of Thoracic and Cardiovascular Surgery*, vol. 149, no. 6, pp. 1622–1628, 2015.
- [21] A. M. Plata, S. J. Sherwin, and R. Krams, "Endothelial nitric oxide production and transport in flow chambers: the importance of convection," *Annals of Biomedical Engineering*, vol. 38, no. 9, pp. 2805–2816, 2010.
- [22] R. Kaunas, H. Kang, and K. J. Bayless, "Synergistic regulation of angiogenic sprouting by biochemical factors and wall shear stress," *Cellular and Molecular Bioengineering*, vol. 4, no. 4, pp. 547–559, 2011.
- [23] L.-D. Jou and M. E. Mawad, "Hemodynamic effect of neuroform stent on intimal hyperplasia and thrombus formation in a carotid aneurysm," *Medical Engineering & Physics*, vol. 33, no. 5, pp. 573–580, 2011.
- [24] T. Meirson, E. Orion, C. Di Mario et al., "Flow patterns in externally stented saphenous vein grafts and development of intimal hyperplasia," *The Journal of Thoracic and Cardiovascular Surgery*, vol. 150, no. 4, pp. 871–879, 2015.
- [25] H. J. Kim, I. E. Vignon-Clementel, J. S. Coogan, C. A. Figueroa, K. E. Jansen, and C. A. Taylor, "Patient-specific modeling of blood flow and pressure in human coronary arteries," *Annals of Biomedical Engineering*, vol. 38, no. 10, pp. 3195–3209, 2010.
- [26] R. Agujetas, M. R. González-Fernández, J. M. Nogales-Asensio, and J. M. Montanero, "Numerical analysis of the pressure drop across highly-eccentric coronary stenoses: application to the calculation of the fractional flow reserve," *Biomedical Engineering Online*, vol. 17, pp. 1–22, 2018.
- [27] C. A. Taylor, T. A. Fonte, and J. K. Min, "Computational fluid dynamics applied to cardiac computed tomography for noninvasive quantification of fractional flow reserve," *Journal of the American College of Cardiology*, vol. 61, no. 22, pp. 2233–2241, 2013.
- [28] I. E. Vignon-Clementel, C. A. Figueroa, K. E. Jansen, and C. A. Taylor, "Outflow boundary conditions for 3D simulations of non-periodic blood flow and pressure fields in deformable arteries," *Computer Methods in Biomechanics and Biomedical Engineering*, vol. 13, no. 5, pp. 625–640, 2010.
- [29] D. Katritsis, L. Kaiktsis, A. Chaniotis, J. Pantos, E. P. Efstathopoulos, and V. Marmarelis, "Wall shear stress: theoretical considerations and methods of measurement," *Progress in Cardiovascular Diseases*, vol. 49, no. 5, pp. 307–329, 2007.
- [30] F. P. Salvuccia, C. A. Perazzob, S. Salles, J. G. Barrac, and R. L. Armentano, "Influence of inlet conditions in wall shear stress distributions of left coronary arteries in patient-specific simulations," in *Mecánica Computacional*, E. Dvorkin, M. Goldschmit, and M. Storti, Eds., vol. XXIX, pp. 5953–5960, Asociacion Argentina, Buenos Aires, Argentina, 2010.
- [31] M. Piccinelli, A. Veneziani, D. A. Steinman, A. Remuzzi, and L. Antiga, "A framework for geometric analysis of vascular structures: application to cerebral aneurysms," *IEEE Transactions on Medical Imaging*, vol. 28, no. 8, pp. 1141–1155, 2009.
- [32] G. D'Ancona, H. L. Karamanoukian, M. Ricci, S. Schmid, J. Bergsland, and T. A. Salerno, "Graft revision after transit time flow measurement in off-pump coronary artery bypass grafting," *European Journal of Cardio-Thoracic Surgery*, vol. 17, no. 3, pp. 287–293, 2000.
- [33] M. Kroll, J. Hellums, L. McIntire, A. Schafer, and J. Moake, "Platelets and shear stress," *Blood*, vol. 88, no. 5, pp. 1525–1541, 1996.
- [34] S.-W. Lee, L. Antiga, and D. A. Steinman, "Correlations among indicators of disturbed flow at the normal carotid bifurcation," *Journal of Biomechanical Engineering*, vol. 131, no. 6, Article ID 061013, 2009.
- [35] A. M. Malek, S. L. Alper, and S. Izumo, "Hemodynamic shear stress and its role in atherosclerosis," *JAMA*, vol. 282, no. 21, pp. 2035–2042, 1999.
- [36] A. Ruiz-Soler, F. Kabinejadian, M. A. Slevin, P. J. Bartolo, and A. Keshmiri, "Optimisation of a novel spiral-inducing bypass graft using computational fluid dynamics," *Scientific Reports*, vol. 7, 2017.
- [37] J. Hwang, M. H. Ing, A. Salazar et al., "Pulsatile versus oscillatory shear stress regulates NADPH oxidase subunit expression," *Circulation Research*, vol. 93, no. 12, pp. 1225–1232, 2003.